

continuum of the  $^2P_{3/2}^{\circ}$  ionization limit. It is therefore not surprising that the cross sections were found to vary rapidly in this region.

The absorption coefficients of argon were measured with a discrete line emission source in the same manner as neon and helium and results are presented in Table II and Fig. 3 with a probable error of about  $50 \text{ cm}^{-1}$ .

Near the  $M_3$  edge, the first ionization limit, two low  $k$ -values were obtained for source lines  $\lambda$  781.2 Å and Orv 779.8 Å. They might be considered as indicative of the magnitude of the photoionization cross section due to the transition of one of the  $3p$ -electrons to the continuous level corresponding to the series limit  $^2P_{3/2}^{\circ}$ . Below the  $M_2$  edge the measured  $k$ -value represents the total contribution of two possible transitions and falls off slowly toward shorter wavelengths. At the  $M_2$  edge the cross section was estimated to be  $3.5 \times 10^{-17} \text{ cm}^2$ .

This may be compared with the photoionization cross section of  $3 \times 10^{-17} \text{ cm}^2$  as calculated by Dalgarno<sup>8</sup> for argon at the spectral head.

In the range between 550 Å and 420 Å, many comparatively large  $k$ -values were found as indicated by crosses above the dashed curve in Fig. 3. They may possibly be explained as due to autoionization near the  $M_1$  edge. In contrast, below this edge the absorption coefficients were found uniformly lower.

In summarizing the results obtained, the variation of the photoionization cross sections of helium, argon, and neon *versus* the energy of the incident photon are shown in Fig. 4.

The continued support of this work by the Office of Naval Research is gratefully acknowledged.

<sup>8</sup> A. Dalgarno, Proc. Phys. Soc. (London) **A65**, 666 (1952).

## Photoionization Efficiencies and Cross Sections in $\text{O}_2$ , $\text{N}_2$ , $\text{CO}_2$ , A, $\text{H}_2\text{O}$ , $\text{H}_2$ , and $\text{CH}_4$

N. WAINFAN, W. C. WALKER, AND G. L. WEISSLER

*Department of Physics, University of Southern California, Los Angeles, California*

(Received October 26, 1954)

The photoionization cross sections of several gases were obtained by making simultaneous measurements of the total absorption cross sections and ionization efficiencies in the wavelength region from 473 Å to 1100 Å. In each case the total absorption cross sections were in agreement with those reported by others. For  $\text{O}_2$ , the ionization cross sections were found to be between 5 and  $30 \times 10^{-18} \text{ cm}^2$ , while those for  $\text{N}_2$  were close to  $23 \times 10^{-18} \text{ cm}^2$  over almost the entire range studied. The ionization cross section of argon at the onset of ionization was compared with the theoretical estimate made by Dalgarno. The long-wavelength limits for photoionization were determined and were found to yield ionization potentials in good agreement with those obtained by spectroscopic and electron impact methods.

### INTRODUCTION

**P**RESENT interest in the physics of the upper atmosphere and in that of gaseous discharges has motivated a renewed effort to measure the photoionization cross sections of several of the permanent gases. For a few gases, such as Ne,<sup>1</sup> A,  $\text{CH}_4$ ,<sup>2</sup> and the alkali metal vapors,<sup>3</sup> these cross sections may be inferred from their total absorption cross sections. However, since in many gases several competing absorption processes may be expected, the most unambiguous results can be obtained only from a direct measurement of the number of ion pairs produced per photon absorbed in the gas.<sup>4,5</sup>

The work reported here was concerned with measure-

ments of the absolute photoionization cross sections and ionization efficiencies of  $\text{O}_2$ ,  $\text{N}_2$ ,  $\text{CO}_2$ , A,  $\text{H}_2$ ,  $\text{H}_2\text{O}$ , and  $\text{CH}_4$  as a function of wavelength between 473 and 1020 Å. Techniques employed in this investigation were essentially the same as those described in an earlier paper containing preliminary results for  $\text{O}_2$  and  $\text{N}_2$ .<sup>6</sup>

### APPARATUS AND PROCEDURE

The equipment employed in this study consisted of three major components, a light source and normal-incidence vacuum monochromator, instruments for determining the absolute light intensity at the exit slit, and an assembly of ion chambers, mounted in a gas-filled experiment chamber behind the exit slit, in which the ionization currents and absorption coefficients were measured. The light source and monochromator have been described previously.<sup>6</sup> A line-emitting light source was used in preference to the frequently employed continuum in order to facilitate the separation of first-

<sup>1</sup> P. Lee and G. L. Weissler, Proc. Roy. Soc. (London) **A219**, 71 (1953).

<sup>2</sup> H. Sun and G. L. Weissler, J. Chem. Phys. (to be published).

<sup>3</sup> Ditchburn, Tunstead, and Yates, Proc. Roy. Soc. (London) **A181**, 386-99 (1943).

<sup>4</sup> F. L. Mohler, Phys. Rev. **28**, 46-56 (1926).

<sup>5</sup> Watanabe, Zelikoff, and Inn, AFCRC Technical Report No. 52-53 (unpublished); also, Phys. Rev. **91**, 1155 (1953); K. Watanabe, J. Chem. Phys. **22**, 1564 (1954).

<sup>6</sup> Wainfan, Walker, and Weissler, J. Appl. Phys. **24**, 1318 (1953).

TABLE I. Monochromator wavelengths.

Nominal wavelength in angstroms	Emission lines included			
	0.6-mm slits Approx resolution 10 Å		0.3-mm slits Approx resolution 5 Å	
473	473.0 AIII 473.9 AIII	476.4 AIII 481.8 AIII		
508	503.6 AII 507.4 OIII 507.7 OIII 508.2 OIII 508.4 AIII 508.6 AIII	508.7 AIII 510.6 AII 511.5 AIII 511.6 AIII 512.8 AIII		
530	525.8 OIII 526.5 AII 529.9 AIII 530.5 AII	532.4 AIII 534.3 AIII 535.6 AIII		
550	547.9 AII 548.8 AII 553.3 OIV 553.5 AIII	554.1 OIV 554.5 OIV 555.1 OII		
575	572.0 AII 573.4 AII 576.7 AII	578.6 AII 580.3 AII		
598	597.7 AII 597.8 OIII 599.6 OIII	600.6 OII 602.9 AII		
627	624.6 OIV 625.1 OIV	625.9 OIV 629.7 OV		
644	641.4 AIII 641.8 AIII 643.3 AIII 644.1 OII	644.6 NII 644.8 NII 645.2 NII		
662	661.9 AII 663.1 O	660.4 NII 666.0 AII		
687	683.3 AIV 684.9 NIII 685.5 NIII	685.8 NIII 686.3 NIII 688.5 AIV	684.9 NIII 685.5 NIII 685.8 NIII	686.3 NIII 688.4 AIV
704	702.3 OIII 702.8 OIII 702.9 OIII	703.8 OIII 704.5 AII 704.3 AIV	702.3 OIII 702.8 OIII 702.9 OIII	703.8 OIII 704.5 AII 704.3 AIV
716	Not resolved		715.6 Av	715.7 Av
720	715.6 Av 715.7 Av 718.1 AII 718.5 OII	718.6 OII 723.4 AII 725.5 AII	718.1 AII 718.5 OII	718.6 OII 723.4 AII
728	Not resolved		725.5 AII	730.9 AII
762	Not resolved		759.4 OV 760.2 OV 760.4 AIV 761.1 OV	761.5 AIV 762.0 OIV 763.3 NIV 764.4 NIII
770	763.1 NIV 769.2 AIII 769.4 OI 772.9 NIII 771.5 NIII	771.9 NIII 772.5 NIII 776.0 NII 779.8 OIV 779.9 OIV	770.3 OI 772.9 NIII 771.5 NIII 771.9 NIII	772.5 NIII 776.0 NII 779.8 OIV 779.9 OIV
787	787.9 OIV 790.1 OIV	790.4 OIV	787.9 OIV 790.1 OIV	790.4 OIV
797	796.7 OII		796.7 OII	
825	Not resolved		822.2 Av 827.1 Av	827.4 Av
833	827.1 Av 827.4 Av 832.8 OII 832.9 OII 833.3 OII	833.7 OIII 834.5 OIII 835.1 OIII 835.3 OIII	832.8 OII 832.9 OIII 833.3 OII 833.7 OIII	834.5 OII 835.1 OIII 835.3 OIII
843	Not resolved		840.0 AIV	843.8 AIV
850	Not resolved		850.6 AIV	
872	Not resolved		871.1 AIII 875.5 AIII	876.1 AI
894	Not resolved		894.3 AI	898.9 OIII
920	915.6 NII 915.9 NII 916.0 NII 916.7 NII 916.8 AII 921.3 OIV	922.0 NV 923.0 NIV 923.2 NIV 923.4 OIV 923.4 NIV	919.8 AII 921.3 OIV 921.4 OIV 922.5 NIV	923.0 NIV 923.2 NIV 923.4 OIV 923.4 NIV
955	955.3 NIV		955.3 NIV	
979	979.8 NIII	979.9 NIII	979.8 NIII	979.9 NIII
991	988.6 OI 988.8 OI 989.8 NII 989.8 NII 990.1 OI	990.2 OI 990.8 OI 991.5 NIII 991.6 NIII	988.6 OI 988.8 OI 989.8 NIII 989.8 NII 990.1 OI	990.2 OI 990.8 OI 991.5 NIII 991.6 NIII

order from higher-order spectral components. For most of the gases studied, the photoionization cross sections were established using two 1.5-cm-long ionization chambers spaced 10 cm apart along the light beam. The ionization currents generated in these ion chambers were between  $10^{-10}$  and  $10^{-13}$  ampere and were measured with a Beckman, Model V, micro-microammeter. A windowless Reeder thermopile having a sensitivity in vacuum of 1.05 microvolts per microwatt was used to determine the photon flux at the exit slit.<sup>7</sup> In addition

<sup>7</sup> D. M. Packer and C. Lock, J. Opt. Soc. Am. 41, 699 (1951); see also, K. Watanabe and E. C. Y. Inn, J. Opt. Soc. Am. 43, 32 (1953).

to this, a 1P28 photomultiplier tube, sensitized to ultraviolet radiation by having it view a fluorescent screen (Sodium Salicylate or Apeizon L grease),<sup>8</sup> was calibrated against the thermopile and used as a secondary radiation detector. Primary and exit slit widths of 0.6 mm each limited the resolution of this system to 10 Å.

In order to provide a check on the accuracy and to eliminate instrumental errors the work was repeated, for several of the gases, using three, 3 cm long, ionization chambers in tandem, each separated by a distance of

<sup>8</sup> Johnson, Watanabe, and Tousey, J. Opt. Soc. Am. 41, 702 (1951).

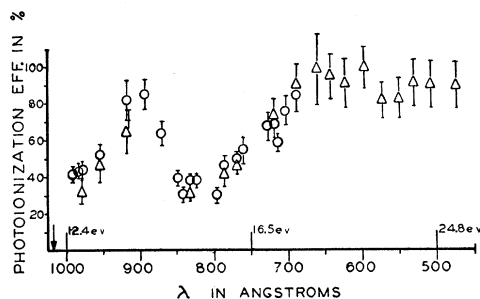


FIG. 1. Photoionization efficiencies of  $O_2$ .  $\Delta$  Data taken with 1.5-cm ion chambers, and 10 Å resolution.  $\circ$  Data taken with 3-cm ion chambers, and 5 Å resolution. The first ionization limit at  $1019 \pm 10$  Å is indicated on the wavelength axis by an arrow.

25 cm. For use in conjunction with these chambers the Reeder thermopile was replaced by one of the Schwarz-Hilger type. Its increased sensitivity of 9.5 microvolts per microwatt in vacuum eliminated the necessity for the photomultiplier tube and permitted the use of 0.3 mm wide slits which gave a 5 Å resolution.

Because of the five- to ten-angstrom resolution of the monochromator, the radiation at each of the nominally assigned wavelengths consisted, in many cases, of a number of individual light source emission lines. Although no detailed identification of these lines was made, spectrograms were taken with a 10-micron wide primary slit and compared with the wavelength table compiled by Boyce and Moore.<sup>9</sup> The possible emission lines falling within each resolved wavelength band are tabulated in Table I. In addition to the line emitting source, a hydrogen glow discharge<sup>8</sup> was used providing a wavelength continuum down to about 900 Å. This light source helped to establish the long wavelength ionization limits in  $O_2$  and  $CH_4$ .

In order to determine both the photoionization efficiencies and cross sections of a particular gas it was first necessary to determine the absolute absorption coefficient  $k$  of the gas. At the working pressure and temperature the value of  $k$  is defined by Lambert's law as follows:  $k = -\ln(I_d/I_0)/d$ . Since the saturated ionization currents are proportional to the intensity of the light beam passing through the ion chambers, this can be written as  $k = -\ln(i_2/i_1)/d$ , where  $i_1$  is the ion current in the ion chamber nearest the exit slit and  $i_2$  is that in another chamber separated a distance  $d$  cm from the first. From a knowledge of  $k$  and the incident photon flux at the exit slit the number of photons per second  $N$  absorbed in the first ion chamber may be obtained as follows:  $N = I_0 \{ \exp[-kX] - \exp[-k(X+L)] \}$ , where  $I_0$  is the photon flux at the exit slit of the gas-filled experiment chamber,  $X$  is the distance between the exit slit and the leading edge of the first ion chamber and  $L$  is the length of the collector electrode for this ion chamber. The photoionization efficiency  $\gamma$ , in per-

cent, can then be calculated from the ratio of the ionization current in charges per second to the number of photons per second absorbed in the ion chamber, that is,  $\gamma = (i_1/N) \times 100$ . The total absorption cross section  $\sigma$ , obtained by dividing the value of  $k$  by Loschmidt's number, can then be combined with the photoionization efficiency to give the cross section for ionization by all processes from the relation  $\sigma_i = \sigma\gamma$ .

Test runs made with the experiment chamber evacuated to a pressure of about  $5 \times 10^{-5}$  mm of Hg, as well as the occurrence of sharp ionization onsets, indicated that photocurrents from the ion chamber walls due to reflected or scattered light were negligible. The remaining possible sources for error in the present investigation, included in calculating the probable errors of the photoionization results presented, were the following: (1) an estimated five percent error in the determination of the absolute light intensity, (2) a five percent calibration error in the current recording system, (3) an error in the absolute pressure measurements, and (4) an error in the measured total absorption coefficients. Since the ionization cross section depended directly on the value of the total absorption coefficient, there was some variation in the accuracy of the results for different lines. The probable errors for each line are indicated in the figures.

## RESULTS AND DISCUSSION

Because of their importance in upper atmospheric physics, the gases  $O_2$  and  $N_2$  were investigated in detail. In addition several less abundant atmospheric components,  $CO_2$ , A,  $H_2$ , and  $H_2O$  were studied, though less extensively. Theoretical interest also motivated a brief consideration of  $CH_4$ .<sup>10</sup>

### Oxygen

Ionization efficiencies and cross sections for  $O_2$  are graphically presented in Figs. 1 and 2 and together

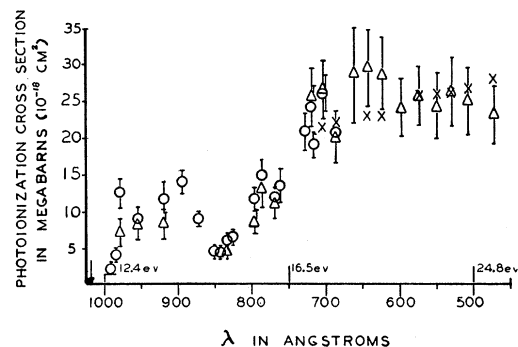


FIG. 2. Photoionization cross sections of  $O_2$ .  $\Delta$  Data taken with 1.5-cm ion chambers.  $\circ$  Data taken with 3-cm ion chambers.  $\times$  Estimate of ionization continuum made by Lee and Weessler (reference 14). The first ionization limit at  $1019 \pm 10$  Å is indicated on the wavelength axis by an arrow.

<sup>9</sup> J. C. Boyce and J. T. Moore, "Provisional Wavelength Identification Tables for the Vacuum Ultraviolet," Massachusetts Institute of Technology, 1941 (unpublished).

<sup>10</sup> A. Dalgarno, Proc. Phys. Soc. (London) **A65**, 663 (1952).

TABLE II. Photoionization in O<sub>2</sub>.

λ	With small ion chambers			With large ion chambers		
	σ <sub>tot</sub> × 10 <sup>18</sup> cm <sup>2</sup>	Eff in %	σ <sub>ion</sub> × 10 <sup>18</sup> cm <sup>2</sup>	σ <sub>tot</sub> × 10 <sup>18</sup> cm <sup>2</sup>	Eff in %	σ <sub>ion</sub> × 10 <sup>18</sup> cm <sup>2</sup>
473	26.0±2.6	88.8±13.2	23.1 ±4.1			
508	27.7±2.8	89.9±13.5	24.9 ±4.5			
530	29.0±2.9	90.3±13.5	26.2 ±4.7			
550	29.3±2.9	82.7±12.4	24.2 ±4.4			
575	31.2±3.1	82.0±10.3	25.6 ±4.1			
598	24.0±2.4	99.8±13.0	23.9 ±4.0			
625	31.5±3.2	90.8±13.6	28.6 ±5.2			
644	31.0±3.1	94.9±14.2	29.4 ±5.3			
662	29.0±2.9	98.4±19.7	28.5 ±6.4			
687	21.9±2.2	90.2±11.7	19.8 ±3.3	24.6 ±1.05	83.9±11.8	20.6 ±3.0
704	33.4±3.3	79.2± 9.5	26.5 ±4.1	34.4 ±1.6	75.6± 6.5	26.0 ±2.5
716				32.5 ±1.6	58.4± 4.5	19.0 ±1.7
720	34.6±3.5	73.7± 8.9	25.5 ±4.0	35.2 ±1.5	68.4± 7.4	24.2 ±2.8
728				31.0 ±1.7	67.4± 7.5	20.8 ±2.6
762				24.9 ±2.1	54.5± 7.3	13.6 ±2.2
770	22.7±2.3	47.8± 5.7	10.9 ±1.7	24.1 ±1.2	49.5± 4.5	11.9 ±1.2
787	31.0±3.1	42.1± 6.3	13.1 ±2.4	32.0 ±1.7	46.7± 5.8	14.9 ±2.0
797	35.2±3.5	23.9± 3.0	8.41±1.4	38.2 ±2.3	30.6± 3.0	11.7 ±1.4
825				16.5 ±1.2	38.2± 3.2	6.30±0.70
833	14.5±1.5	32.3± 3.9	4.67±0.75	15.2 ±0.79	38.7± 2.9	5.88±0.54
843				14.3 ±0.96	31.1± 3.7	4.34±0.61
850				11.4 ±0.84	39.6± 4.5	4.50±0.61
872				14.1 ±0.70	63.2± 7.3	8.91±1.1
894				16.1 ±0.63	84.6± 8.1	14.0 ±1.4
920	12.5±1.9	65.1±13.0	8.17±2.0	14.3 ±1.1	81.8±10.6	11.7 ±2.2
955	17.5±2.6	46.0± 9.2	8.05±2.0	16.9 ±2.5	52.4± 5.5	8.86±1.6
979	22.4±3.4	31.4± 6.3	7.04±1.8	28.1 ±3.9	44.6± 3.3	12.5 ±2.0
985				9.2 ±1.2	42.4± 3.4	3.9 ±0.59
991				4.75±1.5	4.13± 3.7	1.96±0.64
	Av of 2 runs (1 at 100 microns, 1 at 50 microns)			Av of 5 runs (2 at 96 microns, 2 at 44 microns, 1 at 23 microns)		

with the total absorption cross sections are compiled in Table II.

The onset of ionization was found at 1019±10 Å corresponding to an ionization potential of 12.1±0.1 volts.<sup>11</sup> This value was found to be in good agreement with the 12.1±0.20 volts obtained by Hagstrum<sup>12</sup> for the production of O<sub>2</sub><sup>+</sup>-ions by electron bombardment and with the 12.2±0.1 volt result of Price and Collins<sup>13</sup> for the transition O<sub>2</sub> X <sup>3</sup>Σ<sub>g</sub><sup>-</sup>→O<sub>2</sub><sup>+</sup> X <sup>2</sup>Π<sub>g</sub>. Good agreement was also noted between the total absorption cross sections presented and those of Weissler and Lee.<sup>14</sup>

Between the first ionization limit at 1019 Å and the second at 763 Å most of the photoions were produced in the O<sub>2</sub> X <sup>3</sup>Σ<sub>g</sub><sup>-</sup>→O<sub>2</sub><sup>+</sup> X <sup>2</sup>Π<sub>g</sub> transition. The possibility of autoionization cannot be excluded entirely because of the existence of strong molecular absorption bands in this region. However, it was impossible to observe this process separately in the present work. Resonance absorption bands reported by Collins and Price,<sup>18</sup>

<sup>11</sup> The ionization limit presented here is at a slightly longer wavelength than that previously reported by the authors (see reference 6). The present value was obtained after a small error in the wavelength scale of the monochromator had been corrected. It should also be noted that in the previous paper the O<sub>2</sub> ionization limits were stated incorrectly. The correct designations are O<sub>2</sub><sup>+</sup> X <sup>2</sup>Π<sub>g</sub> for the first ionization limit, O<sub>2</sub><sup>+</sup> α <sup>4</sup>Π<sub>u</sub> for the second, and O<sub>2</sub><sup>+</sup> A <sup>2</sup>Π<sub>u</sub> for the third.

<sup>12</sup> H. D. Hagstrum, Revs. Modern Phys. 23, 185-203 (1951).

<sup>13</sup> W. C. Price and G. Collins, Phys. Rev. 48, 714-19 (1935).

<sup>14</sup> G. L. Weissler and P. Lee, J. Opt. Soc. Am. 42, 200-203 (1952).

which were found down to about 680 Å, coincide with the regions of low-ionization efficiencies. The non-ionizing absorbed photons were assumed to excite those molecular states which give rise to these bands. In the region of continuous absorption below 680 Å the high-ionization efficiencies indicated that almost all the absorption occurred by one or more of the energetically possible photoionization processes.

The data for O<sub>2</sub> were obtained for pressures from 23 to 100 microns and within this range the results were found to be independent of the pressure. Thus, it is unlikely that two step ionization events occurred in the gas. In addition the hydrogen glow light source was used to explore the region between the ionization limit and the Lyman α line at 1216 Å. No evidence of two step ionization processes preceding the ionization limit was found although currents down to 3×10<sup>-13</sup> ampere or two orders of magnitude smaller than those measured during the experiment could easily be detected.

### Nitrogen

Figures 3 and 4 show the photoionization efficiencies and cross sections in N<sub>2</sub>. These results in addition to the total absorption cross sections are compiled in Table III.

From an onset at 792±5 Å the ionization efficiency increased rapidly to values near 100 percent at about 700 Å, and at wavelengths shorter than this nearly the

TABLE III. Photoionization in N<sub>2</sub>.

$\lambda$	With small ion chambers			With large ion chambers		
	$\sigma_{\text{tot}} \times 10^{18} \text{ cm}^2$	Eff in %	$\sigma_{\text{ion}} \times 10^{18} \text{ cm}^2$	$\sigma_{\text{tot}} \times 10^{18} \text{ cm}^2$	Eff in %	$\sigma_{\text{ion}} \times 10^{18} \text{ cm}^2$
473	24.5±2.5	84.5±12.7	20.8±3.8			
508	25.0±2.5	88.5±13.3	22.2±4.0			
530	25.8±2.6	89.0±13.4	23.0±4.2			
550	27.1±2.7	86.0±12.9	23.3±4.2			
575	24.1±2.4	87.5±13.1	21.1±3.8			
598	22.4±2.2	101.0±15.0	22.4±4.0			
625	22.7±2.3	101.5±15.0	22.7±4.2			
644	23.8±2.4	93.1±14.0	22.1±4.0			
662	30.3±4.6	99.0±19.8	30.0±7.5			
687	25.7±2.6	88.8±13.3	22.9±4.1	27.4±1.20	82.4±6.2	22.6±2.0
704	24.0±2.4	89.8±13.5	21.5±3.9	25.4±1.04	91.3±9.5	23.0±2.6
716				26.7±1.20	69.5±6.7	18.6±2.0
720	21.4±2.1	100.7±15.1	21.4±3.8	20.1±1.07	80.3±6.6	16.2±1.6
728				37.5±2.9	69.9±7.3	25.5±3.3
762				32.6±3.7	65.0±5.5	21.2±3.0
770	28.5±2.9	50.2± 7.5	14.3±2.6	31.4±3.2	55.5±5.6	17.5±3.0
787	19.3±1.9	45.6± 6.8	8.8±1.6	17.5±3.1	51.5±7.0	9.0±2.0

1 run at 100 microns 3 runs (1 at 102 microns, 1 at 43.5 microns, 1 at 29.0 microns)

entire absorption mechanism appeared to be that of photoionization. The onset limit corresponded to a first ionization potential of  $15.6 \pm 0.1$  volts, which is in good agreement with the  $15.7 \pm 0.2$  volts obtained by

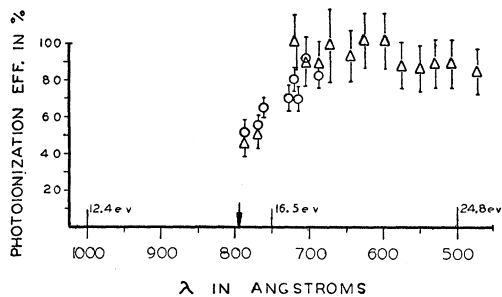


FIG. 3. Photoionization efficiencies of N<sub>2</sub>.  $\Delta$  Data taken with 1.5-cm ion chambers, and 10 Å resolution.  $\circ$  Data taken with 3-cm ion chambers, and 5 Å resolution. The first ionization limit at  $792 \pm 5$  Å is indicated on the wavelength axis by an arrow.

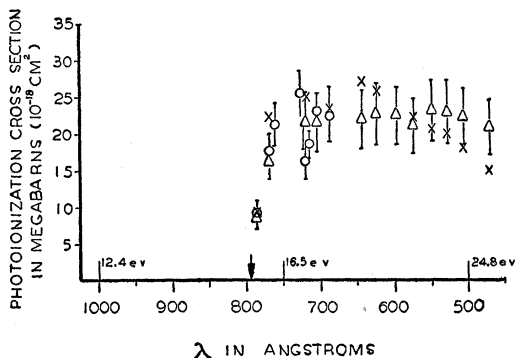


FIG. 4. Photoionization cross sections of N<sub>2</sub>.  $\Delta$  Data taken with 1.5-cm ion chambers and 10 Å resolution.  $\circ$  Data taken with 3-cm ion chambers and 5 Å resolution.  $\times$  Estimate of ionization continuum made by Lee and Weissler (reference 16). The first ionization limit at  $792 \pm 5$  Å is indicated on the wavelength axis by an arrow.

Hagstrum<sup>12</sup> and also with the ionization limit of 796 Å or 15.58 volts for the transition N<sub>2</sub> X  $^1\Sigma_g^+ \rightarrow N_2^+ X \ ^2\Sigma_g^+$  as determined from band spectroscopy.<sup>15</sup> Again as in the case of O<sub>2</sub> the total absorption cross sections agreed with previous results.<sup>16</sup>

Excitation of the  $\sigma_u$  2s-electrons to levels above the first ionization limit made autoionization a possible mechanism in N<sub>2</sub>.<sup>17</sup> Since Hagstrum found no N<sup>+</sup>-ions appearing at electron impact energies less than 24.3 eV corresponding to a wavelength of 508 Å, it was assumed that almost the entire absorption mechanism between 796 and 508 Å involved the production of N<sub>2</sub><sup>+</sup>-ions by the removal of the  $\sigma_g$  2s- or possibly the  $\sigma_u$  2s-electrons from the molecule.

### Carbon Dioxide

Photoionization results for CO<sub>2</sub> are shown in Figs. 5 and 6. An ionization potential of  $14.0 \pm 0.3$  volts corresponding to  $883 \pm 15$  Å was observed for this gas. The relatively large uncertainty of  $\pm 15$  Å in the position of the onset was due to a lack of sufficient light source emission lines near this onset. Within the error limits stated the present result agreed with the  $13.73 \pm 0.01$  volt figure obtained by Price and Simpson<sup>18</sup> from an analysis of the absorption spectrum of CO<sub>2</sub>. Total absorption coefficients, reduced to N.T.P., varying between 300 and 1500 cm<sup>-1</sup> were measured in the region from 473 to 883 Å and were found to be in excellent agreement with recent results obtained by Sun.<sup>19</sup> Between the onset of ionization and 690 Å the rapid fluctuation of the ionization cross sections was pre-

<sup>15</sup> G. Herzberg, *Molecular Spectra and Molecular Structure* (D. Van Nostrand Company, Inc., New York, 1950), p. 459.

<sup>16</sup> Weissler, Lee, and Mohr, *J. Opt. Soc. Am.* **42**, 84 (1952).

<sup>17</sup> E. R. Worley, *Phys. Rev.* **64**, 207 (1943).

<sup>18</sup> W. C. Price and D. M. Simpson, *Proc. Roy. Soc. (London)* **A169**, 501 (1939).

<sup>19</sup> H. Sun and G. L. Weissler, *J. Chem. Phys.* (to be published).

sumably due to the strong molecular absorption bands extending from 1150 to 690 Å.<sup>18</sup> Since the acceptance band of the monochromator included a number of emission lines, the presence of these absorption bands caused a considerable difference between data taken at the two different resolutions.

### Argon

In Figs. 7 and 8 are presented results for argon. The ionization limit found at  $790 \pm 5$  Å, which is equivalent to  $15.7 \pm 0.1$  volts, is in agreement with the 15.76 volt figure listed by Moore.<sup>20</sup> From this threshold the ionization efficiency was observed to rise steeply as would be expected in the case of a monatomic gas. The photoionization cross sections were found to be in good agreement with the estimate of the ionization continuum made by Lee and Weissler.<sup>21</sup> A cross section of  $27 \times 10^{-18}$  cm<sup>2</sup> was found at 770 Å, that is, just beyond the onset. This result agrees with the theoretical estimate made by Dalgarno<sup>10</sup> of  $30 \times 10^{-18}$  cm<sup>2</sup> at the ionization limit. In this comparison, the 770 Å line was chosen since at a 5 Å resolution it was the longest wavelength

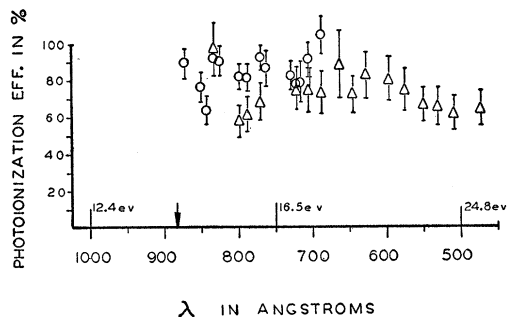


FIG. 5. Photoionization efficiencies of CO<sub>2</sub>.  $\Delta$  Data taken with 1.5-cm ion chambers and 10 Å resolution.  $\circ$  Data taken with 3-cm ion chambers and 5 Å resolution. The first ionization limit at  $883 \pm 15$  Å is indicated by an arrow on the wavelength axis.

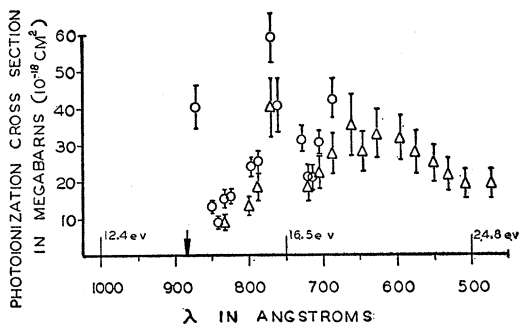


FIG. 6. Photoionization cross sections of CO<sub>2</sub>.  $\Delta$  Data taken with 1.5-cm ion chambers and 10 Å resolution.  $\circ$  Data taken with 3-cm ion chambers and 5 Å resolution. The first ionization limit at  $883 \pm 15$  Å is indicated on the wavelength axis by an arrow.

<sup>20</sup> C. Moore, *Atomic Energy Levels*, National Bureau of Standards Circular No. 467 (U. S. Government Printing Office, Washington, D. C., 1949), Vol. I, p. 211.

<sup>21</sup> P. Lee and G. L. Weissler, *Phys. Rev.* (to be published).

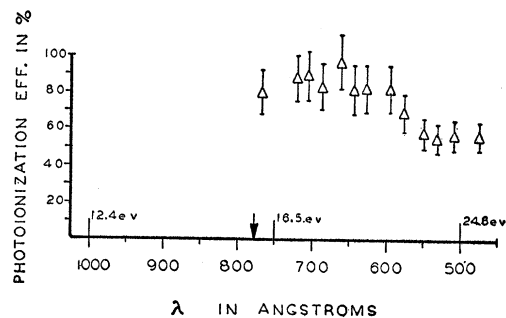


FIG. 7. Photoionization efficiencies of argon.  $\Delta$  Data taken with 1.5-cm ion chambers, and 10 Å resolution. The first ionization limit of  $790 \pm 5$  Å is indicated on the wavelength axis by an arrow.

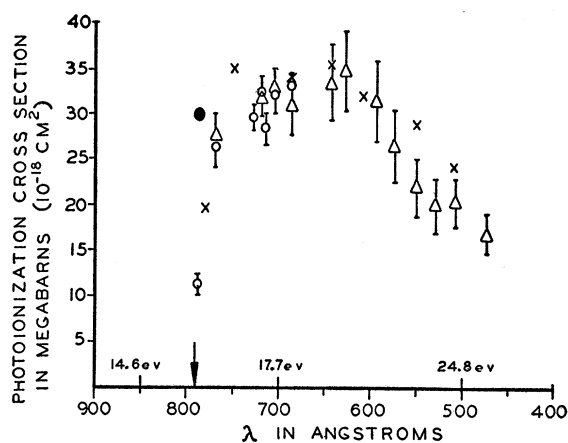


FIG. 8. Photoionization cross sections of argon.  $\Delta$  Data taken with 1.5-cm ion chambers, and 10 Å resolution.  $\circ$  Data taken with 3-cm ion chambers, and 5 Å resolution.  $\times$  Estimate of the ionization continuum made by Lee and Weissler (reference 21).  $\bullet$  Theoretical estimate of Dalgarno (reference 10). The first ionization limit at  $790 \pm 5$  Å is indicated on the wavelength axis with an arrow.

line lying outside the autoionization region of argon. The cross section for this line should therefore correspond to a direct ionization process as assumed by Dalgarno. Within the autoionization region, that is, between 787 Å and 778 Å, a much smaller cross section was observed.

### Hydrogen and Water

Because of the general interest in H<sub>2</sub> and H<sub>2</sub>O preliminary results in these gases are presented in Figs. 9, 10, and 11. Total absorption coefficients for H<sub>2</sub> have been measured by Lee and Weissler<sup>22</sup> who reported values varying between 200 and 500 cm<sup>-1</sup> in the region from the ionization limit at 803.7 Å to 680 Å, a region containing strong absorption bands. The absorption coefficients observed in the present investigation for H<sub>2</sub>, representing averages over a 5 Å band width, were found to fall well within the range reported by Lee and Weissler. It should also be noted that the large ioniza-

<sup>22</sup> P. Lee and G. L. Weissler, *Astrophys. J.* **115**, 570 (1952).

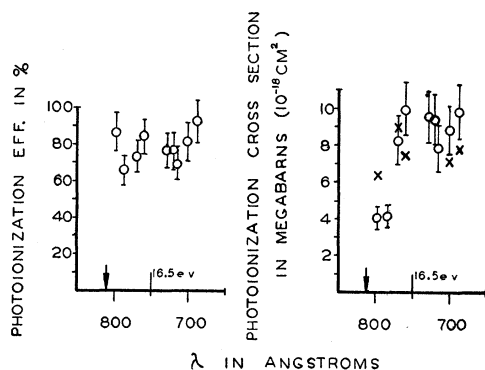


FIG. 9. Photoionization efficiencies and cross sections of  $H_2$ .  $\circ$  Data taken with 3-cm ion chambers, and 5 A resolution.  $\times$  Estimate of the ionization continuum made by Lee and Weissler (reference 22). The first ionization limit at  $810 \pm 15$  A is indicated on the wavelength axis by an arrow.

tion efficiencies obtained for  $H_2$  verified the estimate of the magnitude of the ionization continuum absorption made by these investigators.<sup>22</sup> For  $H_2$  the ionization onset observed was in agreement, within experimental error, with the generally accepted value of 803.7 A.

In the case of  $H_2O$ , the vapor was obtained by sublimation from distilled water ice and its pressure was maintained constant by controlling the temperature of the ice. The total absorption coefficients obtained for  $H_2O$  vapor, using the vapor pressure given by a thermocouple gauge, were compared to the results reported by Astoin, Johannin-Gilles, and Vodar<sup>23</sup> and were found not to agree too well in the wavelength region near 473 A. On the basis of this comparison an estimated probable error of  $\pm 30$  percent, due to the uncertainty in the pressure determination, was placed on the photoionization cross sections presented in Fig. 11. An ionization limit of  $985 \pm 5$  A corresponding to  $12.5 \pm 0.1$  volts was obtained from the position of the ionization onset in  $H_2O$ . This value was in excellent agreement with that obtained by Smith and Bleakney<sup>24</sup> using electron impact techniques.

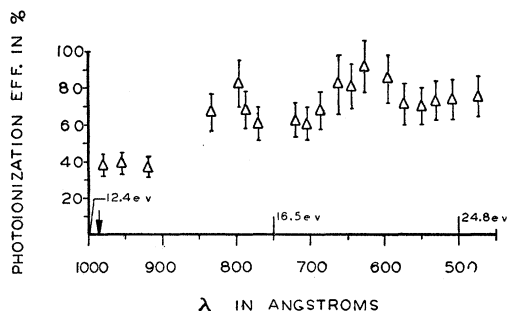


FIG. 10. Photoionization efficiencies of  $H_2O$ .  $\triangle$  Data taken with 1.5-cm ion chambers, and 10 A resolution. The first ionization limit at  $985 \pm 5$  A is indicated on the wavelength axis with an arrow.

<sup>23</sup> Astoin, Johannin-Gilles, and Vodar, *Compt. rend.* **237**, 558-560 (1953).

<sup>24</sup> L. G. Smith and W. Bleakney, *Phys. Rev.* **49**, 883(A) (1936).

## Methane

Preliminary results on photoionization in  $CH_4$  are shown in Fig. 12. Data taken at three pressures of 16.4, 28.5, and 50 microns were found, within experimental error, to be independent of the gas pressure. The total absorption cross sections calculated from these data are presented in Fig. 13 and compared there with the more accurate observations of Ditchburn<sup>25</sup> and of Sun and Weissler in this laboratory.<sup>26</sup> A  $12.8 \pm 0.2$  volt ionization potential, corresponding to 967 A, was obtained which is in accord with the estimate of Sun and Weissler, and with the 12.72 volt value reported by Smith and Bleakney.<sup>24</sup>

In the region from 800 A to 700 A the ionization efficiencies appeared to be larger than 100 percent. Three processes were considered to explain this anomaly; (1) photoelectric emission from the ion chamber walls by photons from the decay of excited states of the ionization products, (2) secondary electron emission by the positive ions collected in the ion chamber, and

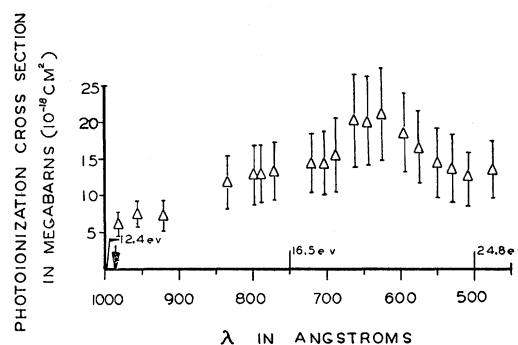


FIG. 11. Photoionization cross sections of  $H_2O$ .  $\triangle$  Data taken with 1.5-cm ion chambers, and 10 A resolution. The first ionization limit at  $985 \pm 5$  A is indicated on the wavelength axis by an arrow.

(3) additional positive ion formation by some type of secondary process in the volume of the gas. An attempt was made to observe the presence of photoemission at the walls by measuring the ionization current with and without opaque shields masking the collector electrode from the region outside the ion chamber. Since no difference in readings was obtained with this arrangement, it was concluded that (1) was not effective in contributing to the increased collection current. The process (2) above could account for only a small fraction of the increased current since it appears that the efficiency for this process at very low energy is only of the order of 1 to 2 percent.<sup>27</sup> Thus it seemed probable that the abnormally large ionization efficiencies observed between 800-700 A were due to positive ion production by some, as yet not identified, secondary

<sup>25</sup> R. W. Ditchburn, *Proc. Roy. Soc. (London)* **A229**, 44 (1955).

<sup>26</sup> H. Sun and G. L. Weissler, *J. Chem. Phys.* (to be published).

<sup>27</sup> J. H. Parker, *Phys. Rev.* **93**, 1148 (1954).

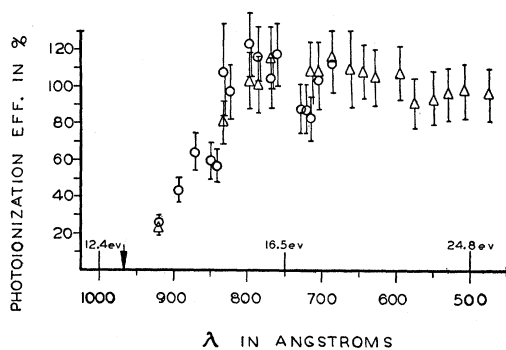


FIG. 12. Photoionization efficiencies of  $\text{CH}_4$ .  $\Delta$  Data taken at 100 microns with 1.5-cm ion chambers, and a 10 Å resolution.  $\circ$  Average of data taken with 3-cm ion chambers at 16.4 and 28.5 microns with a 5 Å resolution. The first ionization limit at  $967 \pm 10$  Å is indicated on the wavelength axis by an arrow.

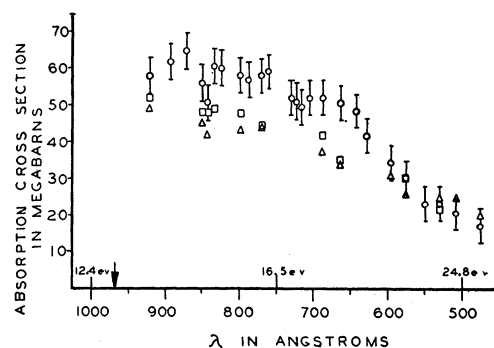


FIG. 13. Absorption cross sections of  $\text{CH}_4$ .  $\circ$  Average of data taken at 50, 28.5, and 16.4 microns.  $\square$  Data of Ditchburn.  $\Delta$  Data of Hsiang Sun and G. L. Weissler. The first ionization limit at  $967 \pm 10$  Å is indicated on the wavelength axis by an arrow.

process in the body of the gas. For the wavelength region below 700 Å where the efficiency is 100 percent the data in Fig. 13 also represent the ionization cross sections. In the region between the onset of ionization and 800 Å the ionization cross sections due to all processes, primary and secondary, can be obtained by combining the absorption cross sections and the ionization efficiencies. It seems clear from this preliminary study that more extensive work is needed in  $\text{CH}_4$  to

clarify the aforementioned anomalies, and to justify comparison with the theoretical results of Dalgarno.<sup>10</sup>

Further work on some of the aforementioned gases and on others is contemplated for the future in order to answer additional as yet unresolved questions.

Our thanks are due to Dr. H. Sun and Dr. Po Lee for many helpful discussions and to the Office of Naval Research for its continued support of the work reported here.